Reaction Chemistry & Engineering

PAPER

Catalytic activity dependence on morphological properties of acidic ion-exchange resins for the simultaneous ETBE and TAEE liquid-phase synthesis

Received 00th January 20xx,
Accepted 00th January 20xx

DOI: 10.1039/x0xx00000x

www.rsc.org/

R. Soto, C. Fité*, E. Ramírez, M. Iborra and J. Tejero

The simultaneous liquid-phase synthesis of 2-ethoxy-2-methylpropane (ETBE) and 2-ethoxy-2-methylbutane (TAEE) has been studied over fifteen commercial acidic ion-exchange resins. Kinetic experiments were carried out in a batch reactor at T=335 K, and initial molar ratios of alcohol to olefins ($R°_{A/O}$) and between olefins ($R°_{C4/C5}$) of 1.1 and 1, respectively. The catalytic activity, measured as intrinsic initial etherification rates, has been found to decrease in the order: Amberlyst™35 > Amberlyst™48 > Purolite®CT-275 > Amberlyst™15 > Purolite®CT-175 > Amberlyst™40 > Amberlyst™36 > Amberlyst™16 > Purolite®CT-482 > Amberlyst™39 > Amberlyst™DT > Amberlyst™45 > Purolite®CT-124 > Purolite®MN-500 > Amberlyst™46. This catalytic activity rank has been related to the morphological properties of the resins in both dry and swollen state. The ratio of acid capacity to specific volume of swollen polymer has been found to be the main catalyst property that determines its activity: the higher the ratio, the higher the activity.

1. Introduction

One of the most consolidated fields of industrial application of acidic ion-exchange resins (IER) as catalysts is the synthesis of tertiary alkyl ethers such as methyl *tert*-butyl ether (MTBE), ethyl *tert*-butyl ether (ETBE), *tert*-amyl methyl ether (TAME) and, in less extent, *tert*-amyl ethyl ether (TAEE). The framework of applications of IER is however much wider, as they are also suitable catalysts for esterification, hydration, alkylation and oligomerization reactions.[1] The understanding of the relationship between catalytic activity and morphological properties of IER is crucial for selecting the best catalyst and operating conditions as well as for designing new catalysts able to improve the process efficiency.

As organic polymers, resins properties depend on the nature of the monomers, the polymerization method, the crosslinking degree and the nature of the functional groups anchored to the polymeric matrix that confer catalytic activity. Resins synthesized by copolymerization of styrene (S) and divinylbenzene (DVB) in aqueous suspension are the most common porous support for IER catalysts.[2] But other aromatic vinyl compounds as vinyl toluene, vinyl naphthalene, vinyl ethylbenzene, methyl styrene, vinyl chlorobenzene and vinyl xylene can be used as co-monomers in the manufacture of polystyrene-based resins. Two main types of porous structures can be created as a result of the porogens and the amount of crosslinking agent (DVB) used during polymerization: microporous and macroreticular matrix. The former is a closed-cell, also called gel-phase, containing micropores, whereas macro-reticular resins present an open-cell with permanent macropores apart from the gel-phase.[3] Macroporous resins are agglomerates of gel-microspheres with smaller nodules than microporous resins that are fussed together forming permanent meso and macropores. Functionalization of such supports provides catalytic activity to the resins. Depending on the foreseen application, functional groups can be acid, basic, redox or even metallic complexes (transition metals).[2] Acidic IER are usually functionalized with sulphuric acid between 363 and 413 K. Sulfonic groups ($-SO_3H$) are therefore the functional groups eventually incorporated to the resin backbone. Different functional groups can be used to give particular properties to the catalyst, for instance, electron attracting groups such as halogens atoms can be used to enhance thermal resistance.[4]

Apart from sulfonic groups concentration, the catalytic activity of a resin depends upon a combination of its morphological properties, which can vary substantially with the composition of the reaction medium. Catalytic activity is directly related to accessibility or ease of compounds to penetrate into the micro and macroporous channels of the resin matrix. Accessibility to the inner resin active sites depends therefore on the nature of the resin backbone (polymeric matrix), and also on the reaction media in which the resin is immersed. Conventional porosimetric methods as mercury intrusion or nitrogen

University of Barcelona. Faculty of Chemistry. Chemical Engineering and Analytical Chemistry Department. Martí i Franqués 1-11, 08028-Barcelona. Spain.
*Corresponding author: fite@ub.edu

adsorption-desorption are seldom used since they provide information only about dry catalysts.[5] A more suitable approach relies on characterization techniques that consider the variation of the morphological properties of the catalyst with the medium nature, providing more reliable information about the actual resin morphology in the working-state. Inverse Steric Exclusion Chromatography (ISEC) technique supplies morphological information about the swollen polymer using an aqueous solution. The technique relies on measurements of elution volumes of a series of standard solutes with known effective molecular sizes through a chromatographic column filled with the investigated polymer material.[6]

Despite the great relevance of etherification processes, IER screening studies are scarce in the open literature,[7–11] more particularly, those applied to the simultaneous syntheses of ethers as ETBE and TAEE. Nonetheless, such process entails potential industrial interest due to process integration and intensification since it can use the mixed C_4 and C_5 olefinic streams from refineries directly, avoiding thus extra separation units. In this study, a screening of fifteen sulfonic IER is performed for the simultaneous liquid-phase syntheses of ETBE and TAEE from pure olefins and ethanol (EtOH). The main aim is to find out the relationships between resins physicochemical properties and their catalytic activity.

2. Experimental

2.1 Apparatus and analysis

The experimental setup consisted of an isothermal 200 mL stirred tank jacketed batch reactor connected in-line to a gas chromatograph (GC, Agilent 6890) equipped with a mass selective detector (MS, Agilent 5973N). The reaction temperature was controlled by a thermostatic bath. The pressure was kept constant at 2.0 MPa with N_2 to exceed the reaction mixture vapour pressure and to impel the samples to the GC. More detailed information about the experimental setup and the analytical method can be found elsewhere.[12]

2.2 Chemicals

In the experimental runs, the initial reactants mixture was prepared with isobutene (IB, >99.9% GC; Air Liquide, Spain), EtOH absolute dry (max. 0.02 wt.% of water; Panreac, Spain) and a mixture of isoamylenes (IA) composed of 2-methyl-2-butene (2M2B, 96% GC) and 2-methyl-1-butene (2M1B, 4% GC; TCI Europe, Belgium). Additionally, some chemical standards were used for the calibration of the chromatographic analysis system: *tert*-amyl alcohol (TAA, >98.0% GC; TCI Europe, Belgium), *tert*-butyl alcohol (TBA, >99.7% GC; TCI Europe, Belgium), ETBE (>99.0% GC; TCI Europe, Belgium), 2M1B (>99.0% GC; TCI Europe, Belgium), and 2M2B (>99% GC; Sigma Aldrich, Germany). TAEE (99.5% GC) was obtained and purified in our lab after successive distillations in a packed column. Besides the mentioned compounds, methanol (MeOH) absolute dry (max. 0.02 wt.% of water; Panreac, Spain) was used for volumetric swelling experiments.

2.3 Catalysts

The following acidic IER were selected because they have a varied array of morphological properties: Amberlyst™15 (A-15), Amberlyst™16 (A-16), Amberlyst™35 (A-35), Amberlyst™36 (A-36), Amberlyst™39 (A-39), Amberlyst™40 (A-40), Amberlyst™45 (A-45), Amberlyst™46 (A-46), Amberlyst™48 (A-48), Amberlyst™DT (A-DT), Purolite®CT-124 (CT-124), Purolite®CT-175 (CT-175), Purolite®CT-275 (CT-275), Purolite®CT-482 (CT-482) and Purolite®MN-500 (MN-500). As water is known to inhibit catalytic activity in etherification reactions,[13] all IER were pretreated in order to remove as much as possible the initial moisture by following the same procedure: 3 h in atmospheric oven at 383 K and then overnight in a vacuum oven at 383 K. This procedure allowed to reduce the catalyst moisture to 3.5 wt.% for A-35.[13] A similar reduction of the initial water content was assumed for the rest of resins. Table 1 gathers a summary of the main physical properties of the tested catalysts. The experiments were carried out with fresh resins. Although resins can undergo deactivation in the industrial reactor by several reasons,[14] it is expected that the morphological properties play the same relative role on the catalytic activity during the whole resin lifespan, which ranges typically from 6 months up to 5 years.[15]

2.4 Experimental conditions and procedure

2.4.1 Volumetric swelling measures

The degree of swelling of a resin immersed in different solvents can be quantified by means of the swelling ratio (*SR*), which can be defined as the ratio of the volume of swollen resin, in a particular solvent, to the volume of dry resin.[16] Graduated test tubes of 50 mL were used in these measurements conducted at room temperature (293 K). 35 mL of solvent were added to 10 mL of dry resin with commercial particle size and after 24 h, SR was determined for each combination of resin and solvent from the final volume of swollen polymer.

2.4.2 Catalytic activity experiments

The selected operating conditions were close to those of industrial etherification processes: temperature of 335 K, and initial molar ratios of alcohol to olefins ($R°_{A/O}$) and between olefins ($R°_{C4/C5}$) equal to 1.1 and 1, respectively. Based on preliminary experiments,[12] the stirring speed was set to 600 rpm and the particle size range used was 0.25-0.4 mm in order to avoid the effects of external and internal mass transfer resistances, respectively. The catalyst load (CL) varied in the range 0.5–2 g, depending on the different expected catalytic activity. Our previous studies with A-35 resin showed that the effect of CL can be discarded at 353 K using this load range,[12] therefore, the effect of CL was assumed negligible in the present work.

Table 1 Main physical properties of tested catalysts

Catalyst	Type	Acid Capacity [eq $H^+ \cdot kg^{-1}$] [a]	DVB [%][b]	Max. Operating T [°C]	Sulfonation type[c]
A-15	macro	4.81	20	120	C
A-16	macro	4.80	12	120	C
A-35	macro	5.36	20	150	O
A-36	macro	5.40	12	150	O
A-39	macro	4.81	8	130	C
A-40	macro	5.20	high	140	O
A-45	macro	3.65	medium	170	S/Cl
A-46	macro	0.87	high	120	S
A-48	macro	5.62	high	140	O
A-DT	macro	3.94	medium	170	S/Cl
CT-482	macro	3.65	low	190	S/Cl
CT-124	micro	5.00	4	130	C
CT-175	macro	4.98	high	145	C
CT-275	macro	5.37	high	145	O
MN-500	macro	2.70	hyper	130	S

[a] Titration against a standard base. [b] Crosslinking degree classification: low (7-12%); medium (12-17%); high (17-25%); hyper (>50%). [c] Conventionally sulfonated (C), oversulfonated (O), surface sulfonated (S) and sulfonated/chlorinated (S/Cl).

The initial mixture of EtOH, IB and IA was placed into the reactor, pressurized to 1.0 MPa with N_2 and heated up to the desired reaction temperature. The sieved and weighted mass of dry catalyst was injected into the reactor and the pressure was set to 2.0 MPa. That instant was considered the starting time for each run. Samples were taken in-line at different reaction times and analysed by GC/MS. The typical duration of the runs for all tested catalysts was 9 h.

2.5 Calculations and experimental uncertainty

For each sample, conversion of reactant *j* (X_j), selectivity (S_j^k) and yield (Y_j^k) towards product *k* were calculated as follows:

$$X_j = \frac{\text{reacted mole of } j}{\text{initial mole of } j} \quad (1)$$

$$S_j^k = \frac{\text{produced mole of } k}{\text{reacted mole of } j} \quad (2)$$

$$Y_j^k = X_j \cdot S_j^k \quad (3)$$

Etherification rates can be estimated at every instant from the derivative of the mole evolution curve of each ether at that time, according to the definition:

$$r_k = \frac{1}{W_{cat}} \left(\frac{dn_k}{dt} \right)_t \quad (4)$$

where r_k is the reaction rate of formation of the product *k* at time *t*, W_{cat} is the dry catalyst mass, and n_k are the mole of product *k*. The mole evolution curve of each ether was obtained by fitting exponential type equations of the form $n_k = a(1-\exp(-bt))$ to experimental values, *a* and *b* being the fitted parameters. Initial reaction rates (r^0_k) were calculated as the derivative of the fitted mole evolution at the initial instant (t=0). Initial turnover frequency (TOF^0_i) of the catalysts expressed as [$mol \cdot h^{-1} \cdot eq^{-1}$] were estimated as the ratio of r^0_k to the acid capacity.

Experiments using A-35 were replicated and an experimental uncertainty of 6% in mole basis was estimated at a 95% confidence level. The same error order of magnitude was assumed for non-replicated experiments. The mass balance was fulfilled within ±5% in all the runs. As for volumetric swelling experiments, the run with CT-124 was triplicated and an experimental uncertainty of 4% was estimated in volume basis. In consideration of these outcomes, the reproducibility and reliability of the experiments was assured.

3. Results and discussion

3.1 Volumetric swelling tests

The swelling ratio (*SR*) determined in different solvents and the dry bed densities for each IER are gathered in Table 2. Several factors are involved in the swelling phenomenon as the nature of the solvent (polar or non-polar), the resin crosslinking degree, the nature of the functional groups and its concentration.[16] All tested resins swelled in contact with solvents though in very different extent. In agreement with literature,[1,16] water was found to be the solvent that produced the largest swelling for all IER. *SR* values obtained were slightly higher in water than in MeOH and EtOH, indicating that resins swelling in water and in C_1-C_2 alcohols are comparable. On the contrary, non-polar solvent (namely composed by ETBE and 2M2B) produced notably lower values of *SR* for all IER tested. Therefore, it can be concluded that the more polar the solvent, the larger the swelling observed. The largest *SR* values were determined for CT-124 and A-39. As the crosslinking degree of A-39 is the lowest among macroporous resins evaluated and CT-124 is a gel-type resin, it can be inferred that the higher the

crosslinking degree, the lower the expected swelling, and thus, the stiffer the resin structure. Resins with very low acid capacity like A-46, swelled in a lesser extent that other resins with similar crosslinking degree and higher acid capacity (e.g. A-35 or A-48). Comparing conventionally sulfonated resins A-15 and CT-175 with their oversulfonated versions A-35 and CT-275, larger *SR* values are observed for the oversulfonated resins. Hence, the extent of swelling of a resin increases with the acid capacity, which can be explained by repulsion forces caused by extra electrostatic charges provided by an increase of sulfonic groups. Similar *SR* was observed for chlorinated resins (A-45, A-DT and CT-482) and macroreticular oversulfonated resin A-36.

3.2 Characterization of IER

As shown in Table 1, tested IER are all macroreticular, except CT-124, which is a full gel-type resin without permanent meso or macropores. A-35, A-36, A-40, A-48 and CT-275 are oversulfonated resins. A-15, A-16, A-39, CT-124 and CT-175 are conventionally sulfonated resins. A-45, A-DT and CT-482 are chlorinated and sulfonated resins. A-46 and MN-500 are surface sulfonated resins. The limit of conventional sulfonation for a styrenic resin is one sulfonic group per benzene ring,[17] which for a resin with medium crosslinking degree roughly corresponds to 4.5 eq $H^{+}\cdot kg^{-1}$.[18] In resins with such an acid capacity, the acid sites distribution in the catalyst particle is nearly homogeneous, but for resins with lower acid capacity, sulfonation is restricted to the outer layers since sulfonation proceeds from the external to internal layers of the particle.[18]

Fig. 1a shows the N_2 adsorption-desorption isotherms of A-35, CT-482, and CT-124 at 77 K, as examples of macro (oversulfonated and sulfonated/chlorinated) and micro types of IER. N_2 adsorption isotherms of macroporous resins are type II, typical of macroporous solids. In these isotherms, the inflection point or knee takes place near the saturation of the first adsorbed monolayer and with increasing relative pressure, second and higher layers are completed until the number of adsorbed layers becomes infinite.[19] Macroporous resins as A-35 or CT-482 generally show type H1 hysteresis corresponding to solids formed by aggregates of spherical particles.[20] Microporous materials as CT-124 show type I isotherms corresponding to gases adsorbing in microporous solids with pore sizes comparable to adsorbate molecular diameter. The pore volume for CT-124 is naught compared to those of A-35 or CT-482. Pore volume of CT-482 is less than a half of that of A-35. BJH analysis from desorption curve is shown in Fig. 1b for A-35, CT-124 and CT-482. Curves for A-35 and CT-482 show unimodal distribution in the meso and macroporous region with a maximum above 500-600 Å, in agreement with the literature.[21] CT-124 exhibits so low pore volume that these values can be associated with a high level of uncertainty.

As it is well known, morphology of macroreticular resins can be modified as a result of swelling in polar media with the development of non-permanent meso and macropores. A reliable description of the actual pore structure in polar media can be obtained by means of the ISEC technique. The cylindrical pore model allows to characterize macro and mesopores (pore diameter and volume), but not to describe the spaces between polymer chains formed by aggregates and nodules swelling. The geometrical model developed by Ogston[22] gives a good approach of the three-dimensional network of swollen polymer describing micropores as spaces

Table 2 Swelling ratios obtained in different solvents and dry resin bed densities

Catalyst	SR in solvents				Dry bed density [g mL^{-1}]
	Water	Ethanol	Methanol	Solvent [a]	
A-15	1.70	1.60	1.50	1.40	0.61
A-16	2.35	2.35	2.00	1.60	0.88
A-35	1.93	1.85	1.70	1.50	0.65
A-36	2.35	2.35	2.25	1.65	0.91
A-39	3.60	3.22	3.00	1.70	0.92
A-40	1.95	1.90	1.85	1.15	0.86
A-45	2.35	2.35	2.45	1.20	0.85
A-46	1.20	1.20	1.20	1.30	0.46
A-48	1.95	1.85	1.90	1.50	0.68
A-DT	2.30	2.40	2.00	1.15	0.91
CT-124	3.65±0.15	3.10	2.95	1.10	0.90
CT-175	1.70	1.65	1.60	1.40	0.54
CT-275	1.90	1.80	1.85	1.50	0.60
CT-482	2.25	2.10	2.10	1.15	1.10
MN-500	1.40	1.40	1.35	1.35	0.48

[a]Solvent composition (mol.%): IB (0.7), EtOH (0.1), 2M1B (3.0), 2M2B (58.8), ETBE (37.4)

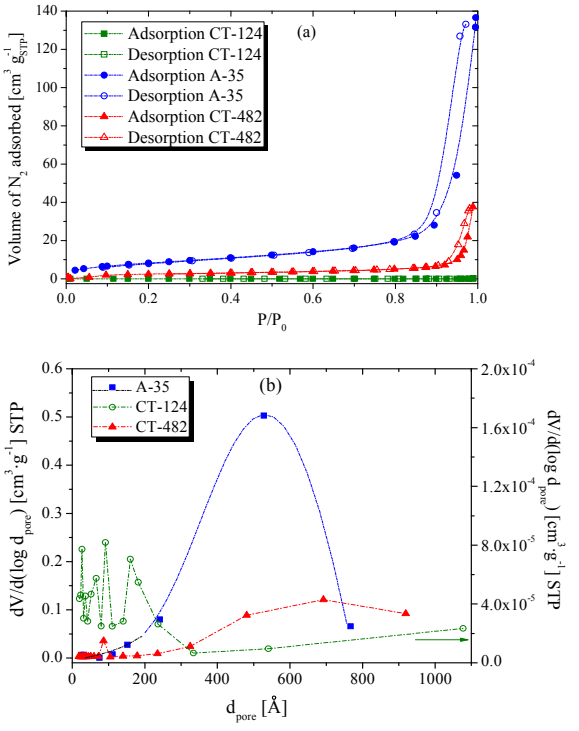

Figure 1 (a) Nitrogen adsorption-desorption isotherms at 77 K for A-35, CT-482 and CT-124. (b) Pore size distribution from N_2 desorption curve for A-35 and CT-482 (left Y axis), and CT-124 (right axis).

between randomly oriented rigid rods. This model also differentiates among zones of swollen gel-phase with different density of polymer chain concentration. The density of polymer chains is described as the total rod length per unit of volume. The distinctive parameter of this model is the specific volume of swollen polymer (V_{sp}) defined as the volume of free space plus the skeleton volume. From ISEC data, Ogston model enables the estimation of V_{sp} and also to distinguish gel zones of different density or characteristic polymer chain concentration. Particularly, for ISEC results in this study, V_{sp} has been modelled into five domains of characteristic polymer chains concentration of 0.1. 0.2, 0.4, 0.8 and 1.5 nm·nm^{-3} for which the spaces between chains are equivalent to pore diameters of 9.8, 4.3, 2.6, 1.5 and 1 nm, respectively.[5] The final ISEC output of the morphology of swollen resin consists of information on both, the distribution of "true pore" (meso and macropores) and the volume distribution of the differently dense gel fractions of the swollen polymer.

The main morphological properties obtained from adsorption-desorption of N_2 in dry polymer state at 77 K, and those obtained in swollen polymer state by ISEC method are presented in Table 3, where the values of polymer density obtained by helium displacement are also included.

As a rule of thumb, the higher the acid capacity, the higher the skeletal density of the polymer. With regards to the properties in dry state (Table 3), the hypercrosslinked resin MN-500 has the highest value (332 m^2g^{-1}) of BET surface area. Macroporous resins with high crosslinking degree showed also high values of BET surface area (from 20 to 60 m^2g^{-1}). The lowest values of BET surface area correspond to microporous resin CT-124 and the low crosslinked resin A-39. This confirms that gel-type resins do not show significant porous structure in dry state, and that crosslinking degree is directly related to the final catalyst BET surface area. Comparing conventionally sulfonated resins CT-175 and A-15 with their oversulfonated versions CT-275 and A-35, it is seen that the conventionally sulfonated ones present higher BET surface area than their oversulfonated versions. With respect to the pore volumes in dry state, they ranged from $2.86\cdot10^{-4}$ to 0.64 cm^3g^{-1}, being MN-500 the resin with the largest pore volume. CT-124 and A-39 exhibited exiguous pore volumes, in agreement with the surface area results. The mean average pore diameter obtained for the studied resins in dry state is within the range 10.9-152 nm.

Concerning the morphological properties obtained by ISEC (Table 3), V_{sp} values ranged from 0.44 to 1.9 cm^3g^{-1}. In agreement with volumetric swelling experiments, gel-type resin CT-124 and low crosslinked resin A-39 showed the highest values of V_{sp} confirming from ISEC technique that swelling phenomenon is more relevant for gel-type resins. Generally, V_{sp} decreased on increasing crosslinking degree for macroreticular resins. "True pores" (meso and macropores)

Table 3 Morphological properties of IER evaluated in dry and swollen states.

Catalyst	Skeletal density	Dry state: adsorption-desorption of N_2[b]				Swollen state polymer (ISEC)[g]				
		Surface area	Pore volume	Pore diameter	Porosity	"True pores"			Gel phase	
	ρ[a] [g cm^{-3}]	$S_{g,BET}$[c] [m^2 g^{-1}]	V_{pore}[d] [cm^3 g^{-1}]	d_{pore}[e] [nm]	θ[f] [%]	$S_{g,ISEC}$ [m^2 g^{-1}]	$V_{pore,ISEC}$ [cm^3 g^{-1}]	$d_{pore,ISEC}$[e] [nm]	V_{sp}[h] [cm^3 g^{-1}]	θ_{ISEC}[i] [%]
A-15	1.416	42.0	0.33	31.2	31.7	156.9	0.63	16.1	0.77	49.5
A-16	1.401	1.7	0.01	30.8	1.8	149.3	0.38	10.3	1.13	52.8
A-35	1.542	34.0	0.21	24.7	24.5	198.9	0.72	14.5	0.61	51.3
A-36	1.567	21.0	0.14	27.2	18.3	146.5	0.33	9.1	1.03	53
A-39	1.417	0.1	$2.86\cdot10^{-4}$	12.7	0.0	56.0	0.16	11.1	1.62	60.3
A-40	1.431	0.2	$6.00\cdot10^{-4}$	10.9	0.1	11.0	0.13	45.5	0.44	–
A-45	1.466	49.0*	0.23	19.0*	25.4	220.2	0.52	9.5	0.97	54.4
A-46	1.137	57.4	0.26	18.3	23.0	186.0	0.48	10.3	0.52	12.3
A-48	1.538	33.8	0.25	29.5	27.7	186.0	0.57	12.3	0.62	45.3
A-DT	1.477	36.0*	0.20	22.0*	22.6	175.4	0.42	9.6	0.97	51.3
CT-124	1.420	0.1	$6.20\cdot10^{-4}$	35.7	0.1	0	0	0	1.90	62.9
CT-175	1.498	28.0	0.30	42.9	31.0	157.4	0.82	20.9	1.00	63.5
CT-275	1.506	20.3	0.38	74.4	36.2	209.4	0.77	14.7	0.81	57.9
CT-482	1.538	8.7	0.06	26.7	8.2	214.0	1.05	19.6	0.85	65.7
MN-500	1.539	332.0*	0.64*	152.0*	50.0	95.8	0.80	33.4	0.89	61.6

[a] Skeletal density. Measured by Helium displacement (Accupic 1330). [b] Samples dried at vacuum (10^{-4} mmHg, 110°C). [c] Brunauer-Emmett-Teller (BET) method. [d] Volume of N_2 adsorbed at relative pressure (P/P_0)=0.99. [e] $d_{pore} = 4V_{pore}/S_{g,BET}$; $d_{pore,ISEC} = 4V_{pore,ISEC}/S_{g,ISEC}$ [f] $\theta = V_{pore}/V_{particle} = V_{pore}/(V_{pore}+1/\rho)$. [g] Measured with 0.2N aqueous solution of Na_2SO_4 as mobile phase, except for MN-500, where THF was used as mobile phase. [h] True volume of swollen polymer. [i] $\theta_{ISEC} = V_{pore,ISEC}/V_{particle} = (V_{pore,ISEC} + V_{sp} - 1/\rho)/(V_{pore,ISEC} + V_{sp})$. *Manufacturer values.

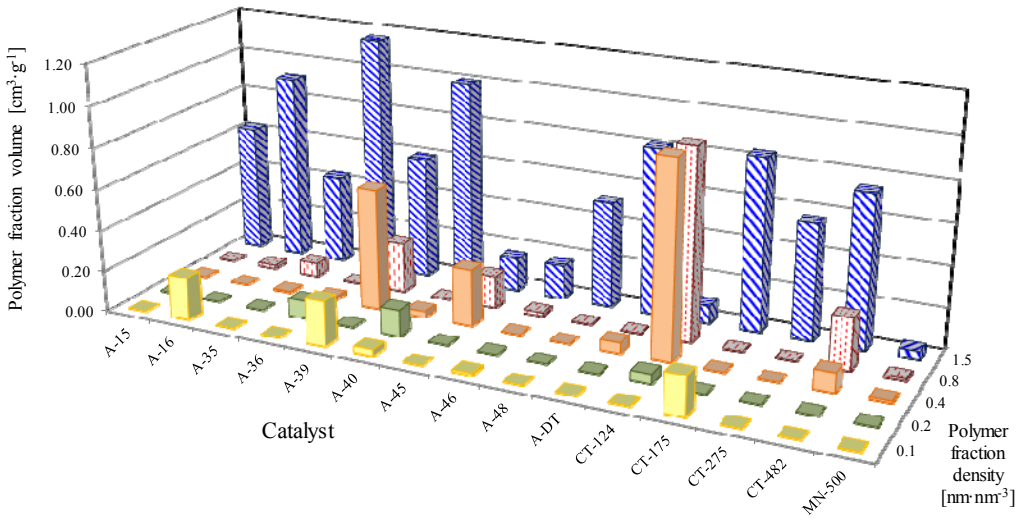

Figure 2 Characterization of the polymer fractions of the assayed catalysts

surface areas obtained by ISEC are notably larger than those obtained in dry state, as well as the pore volumes. This reinforces that resins swelling in polar media affect not only the resins gel-phase but also the morphology of the permanent pores.

Comparing dry and swollen state morphology values for A-16 and A-39, the absence of macropores in dry state is clear. However, new pores are detected when swollen in aqueous media, with surface areas of 149 and 56 m^2g^{-1}, respectively. This supports the abovementioned statement about the formation of new intermediate pores (meso and macropores) for macroporous resins in swollen state. On the other hand, neither meso nor macropores appeared in aqueous media for fully gel-type resin CT-124. Mean pore diameters of resins in swollen state are larger than those estimated in dry state, as expected from the higher pore volume in aqueous media. In addition, porosity values estimated from data in swollen state are generally larger than those estimated from data in dry state. Finally, results obtained for the resin A-40 in both dry and swollen state suggest an anomalous behaviour of this resin. Since A-40 is a macroreticular resin with high crosslinking degree, the very low value of surface area exhibited in the dry state are unusual. Moreover, the value of "true pores" surface area obtained from ISEC is closer to that expected for a microporous resin. A possible explanation is that the resin structure collapsed in the pre-treatment due to thermal creep and fatigue.

The polymer density zone distributions of the swollen gel-phase obtained by ISEC for the tested IER are shown in Fig. 2. As a whole, the densest polymer fraction (1.5 $nm·nm^{-3}$) is generally the most frequent, particularly for macroreticular resins. Gel-type resin CT-124 and low-crosslinked resin A-39 showed important contributions of the zones with medium density (0.4 and 0.8 $nm·nm^{-3}$) to the total polymer volume in aqueous media. As it can be seen, the low polymer fraction volumes of MN-500 confirm the resistance of this resin to swelling according to its extremely high crosslinking degree (50%) and the ensuing stiffness of its structure. Comparing conventionally sulfonated resins CT-175 and A-15 with their respective oversulfonated versions CT-275 and A-35, the former present larger contributions of the densest polymer zone to the total gel-phase volume of swollen polymer. However, A-16 and A-36 showed the opposite trend.

3.3 Conversion, selectivity and yield

As the experimental conditions of the present study were chosen to avoid olefins dimerization,[13,23] the complete product distribution obtained in all the runs is explained by the simplified scheme of parallel reactions presented in Fig. 3. The main reactions R1, R2 and R3 are the etherification of EtOH with IB, 2M1B and 2M2B, respectively. R4 is the double bond isomerization reaction between 2M1B and 2M2B. As a result of the remaining water content in the IER after pretreatment and the low water content of EtOH used as reactant, hydration of IB, 2M1B and 2M2B also took place by means of reactions R5, R6 and R7, respectively, originating TBA and TAA.

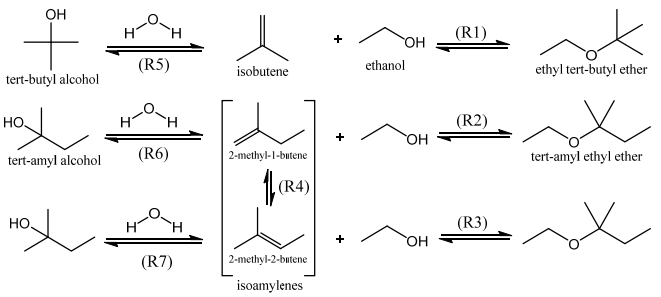

Figure 3 Scheme of the reaction network

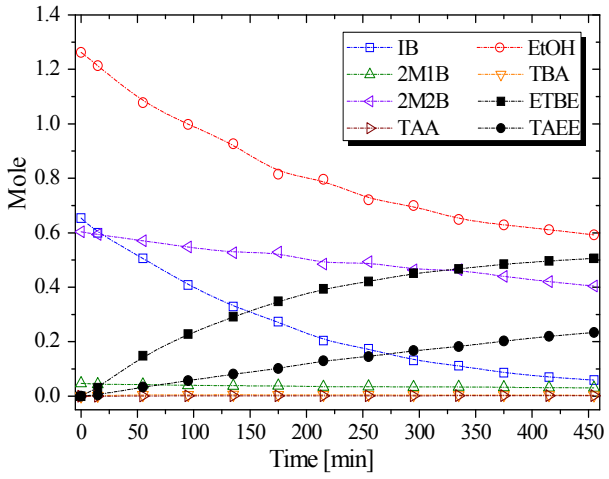

Figure 4 Mole evolution (1g of CT-175, T=335 K, $R°_{A/O}$=1.1 and $R°_{C4/C5}$=1)

Fig. 4 depicts the mole evolution obtained in a typical experiment, in this case for CT-175. All the tested IER were active for the simultaneous syntheses of ETBE and TAEE. According to initial concentrations and thermodynamics of involved reactions,[24] ETBE was the main product in all runs and its formation was faster than that of TAEE for all IER. The amountof tertiary alcohols formed was very similar for all IER and so low that etherification reaction rates can be considered to be non-affected by olefins hydration reactions. The molar fractions of TBA and TAA were always lower than 0.0033 and 0.0015, respectively. The trends in evolution of the reaction medium composition were similar for all tested resins.

Aiming to compare resins, Fig. 5 plots reactants conversion vs. contact time [$\text{min}\cdot g_{cat}\cdot \text{mol}_{EtOH,0}^{-1}$] for all IER evaluated. IB was the reactant that reached the highest conversion level, being close to equilibrium conversion for the most active resins. IB, EtOH and IA conversions at equilibrium under the assayed experimental conditions are 92%, 67% and 54%, respectively.[23,24] As expected, X_{EtOH} was between X_{IB} and X_{IA}. The shape of reactants conversion evolution was similar and three subgroups of resins are distinguished according to the activity level (high, medium and low), as clearly observed in Figs. 5a and 5b. High active resins were macroreticular oversulfonated and conventionally sulfonated resins (A-15, A-16, A-35, A-36, A-40, A-48, CT-175 and CT-275). Medium activity resins were chlorinated, gel-type and macroreticular with low crosslinking degree (A-39, A-45, A-DT, CT-124 and CT-482). Finally, surface sulfonated resins (A-46 and MN-500) showed the lowest activity level.

With respect to reactants selectivity towards products, S_{IB}^{ETBE} and S_{IA}^{TAEE} were larger than 99.7% for all tested resins. Neither olefins dimerization nor further oligomerization products were detected even for the most active catalyst at the end of the runs. Fig. 6a plots EtOH selectivities vs. X_{EtOH} for three resins, as representatives of highly, medium and low activity types described before. The shape of this plot followed identical trends for the rest of resins. EtOH was far more selective towards ETBE than towards TAEE in the first steps of reaction for all IER, but this difference was progressively reduced with the course of reaction. Regarding reactants yield towards products, Fig. 6b depicts the yield evolution obtained for CT-175. Reactants yield towards TAEE increased almost linearly with contact time. The olefins yield to tertiary alcohols was almost null. The shape of the yield evolution was very similar for the rest of IER, being always Y_{IB}^{ETBE} the highest yield reported. To compare data for all IER properly, Table 4 shows a summary of conversion and yield at a fixed contact time of 150 [$\text{min}\cdot g_{cat}\cdot(\text{mol}_{EtOH,0})^{-1}$].

3.4 Etherification reaction rates and turn over frequencies (TOF)

Initial etherification rates were calculated as mentioned in Section 2.5. Table 5 summarizes initial etherification rates and TOF^0 obtained for each IER. *TOF* is an interesting and widely used parameter in catalysis since it gives an idea of the mole converted per active site.

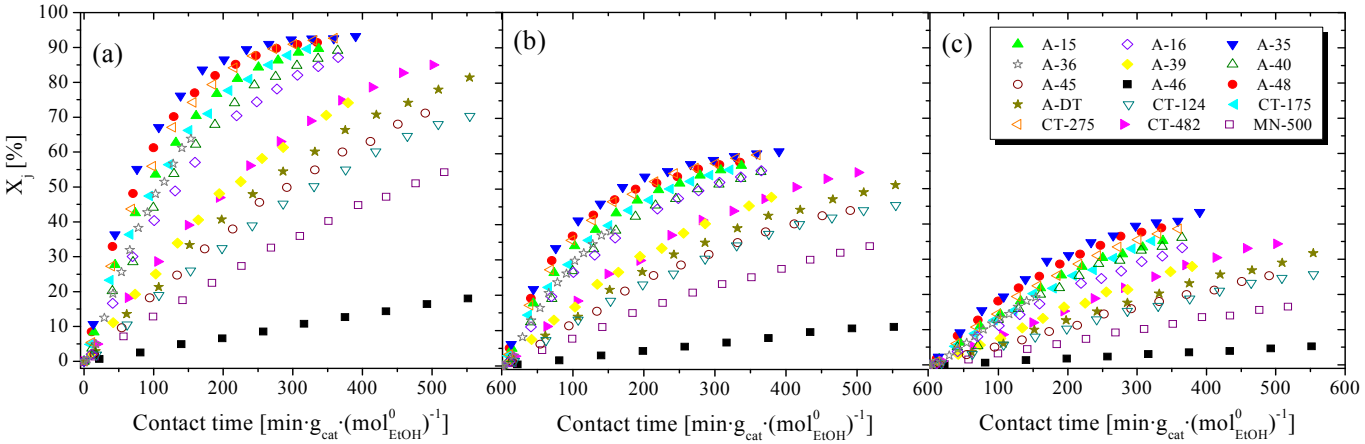

Figure 5 (a) IB , (b) EtOH, and (c) IA conversion vs. contact time for different resins at T=335 K, $R°_{A/O}$=1.1 and $R°_{C4/C5}$=1

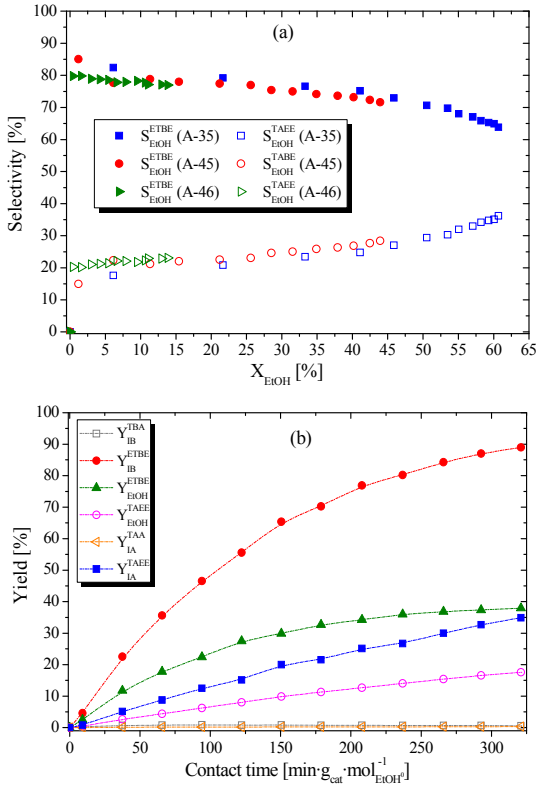

Figure 6 (a) EtOH selectivity vs. X_{EtOH} for A-35, A-45 and A-46. (b) Yield of reactants towards products vs. contact time (1g of CT-175 at T=335 K, $R°_{A/O}$=1.1 and $R°_{C4/C5}$=1)

Table 4 Conversion of reactants and yield to products (T= 335 K, $R°_{A/O}$=1.1 and $R°_{C4/C5}$=1) at the contact time of 150 min·g$_{cat}$·(mol$^{0}_{EtOH}$)$^{-1}$

Catalyst	X_{IB}	X_{EtOH}	X_{IA}	Y_{IB}^{TBA}	Y_{IB}^{ETBE}	Y_{EtOH}^{ETBE}	Y_{EtOH}^{TAEE}	Y_{IA}^{TAA}	Y_{IA}^{TAEE}
A-15	68.4	37.2	21.4	0.2	68.1	28.1	10.4	0.1	23.3
A-16	56.0	33.3	17.1	0.4	55.5	26.9	9.7	0.1	16.8
A-35	78.3	48.5	25.5	0.4	78.0	33.7	13.3	0.3	25.0
A-36	62.5	37.5	18.6	0.3	62.2	28.1	9.4	0.1	18.6
A-39	39.0	23.1	12.6	0.5	38.3	18.8	6.4	0.1	11.2
A-40	60.2	38.0	18.4	1.1	57.2	26.8	11.3	0.3	15.6
A-45	30.5	19.4	7.9	0.3	30.0	14.0	4.0	0.1	7.7
A-46	4.9	3.1	1.4	0.1	4.9	2.5	0.7	0.0	1.4
A-48	75.7	45.2	26.0	0.7	72.9	32.5	12.1	0.2	21.9
A-DT	31.7	21.8	9.2	0.4	30.9	15.5	4.7	0.1	9.2
CT-124	24.1	17.5	10.0	0.4	25.7	13.5	3.9	0.1	9.8
CT-175	66.7	41.6	16.5	0.7	62.6	32.6	10.3	0.0	18.1
CT-275	70.7	45.3	19.5	0.4	74.2	33.2	11.6	0.1	21.4
CT-482	39.2	25.4	12.1	0.4	39.1	17.3	5.6	0.2	11.9
MN-500	18.8	10.1	4.7	0.6	18.1	10.0	2.5	0.1	4.7

As seen in Table 5, A-35 was the most active resin in the simultaneous synthesis of both ethers. On the contrary, A-46 was the least active resin. A-46 presents an especially low acid capacity since sulfonation is restricted to only the first outer few layers of styrene rings in the gel-phase. Globally, oversulfonated and conventionally sulfonated macroreticular IER (A-15, A-35, A-48, CT-175 and CT-275) reported the fastest r^0_{ETBE} and r^0_{TAEE}. Gel-type resin CT-124 showed an activity level

Table 5 Initial etherification rates and TOF^0 for the IER tested. T=335 K, $R°_{A/O}$=1.1 and $R°_{C4/C5}$=1

Catalyst	r^0_{ETBE} [mol·h^{-1}·kg^{-1}]	r^0_{TAEE} [mol·h^{-1}·kg^{-1}]	r^0_{ETBE} / r^0_{TAEE}	TOF^0_{ETBE} [mol·h^{-1}·eq^{-1}]	TOF^0_{TAEE} [mol·h^{-1}·eq^{-1}]
A-15	223.30	47.89	4.66	46.42	9.96
A-16	149.41	34.80	4.29	31.13	7.25
A-35	299.53	70.14	4.27	55.88	13.09
A-36	153.47	38.37	4.00	28.42	7.11
A-39	87.25	24.27	3.60	18.14	5.05
A-40	161.51	39.30	4.11	31.06	7.56
A-45	63.00	16.55	3.81	17.28	4.54
A-46	10.18	3.21	3.17	11.70	3.69
A-48	276.05	62.93	4.39	49.12	11.20
A-DT	74.05	19.47	3.80	18.78	4.94
CT-124	58.97	16.44	3.59	11.79	3.29
CT-175	200.13	41.34	4.84	40.19	8.30
CT-275	249.97	51.69	4.84	46.55	9.62
CT-482	94.42	24.58	3.84	25.85	6.73
MN-500	39.71	10.68	3.72	14.71	3.96

comparable to that of macroporous chlorinated resins with lower acid capacity (A-45 and A-DT). On one hand, this result confirms that etherification reactions take place within the resins gel-phase, where most of the active sites are located. On the other, it suggests that the main role of macropores is to provide spaces that facilitate the accesibility to the actives sites located within the inner part of the polymer, which increases the relative efficiency of active sites (TOF). This macropore feature is evidenced by the notably lower activity of the gel-type resin CT-124 compared to the macroreticular resins as A-15 or CT-175, despite having almost the same acid capacity. The increasing rank of activity was maintained for r^0_{ETBE} and r^0_{TAEE}, indicating that the most active resins for ETBE formation are also the most active for TAEE one. It was: A-46 < MN-500 < CT-124 < A-45 < A-DT < A-39 < CT-482 < A-16 < A-36 < A-40 < CT-175 < A-15 < CT-275 < A-48 < A-35. This is coherent due to the similar chemical nature of both etherification systems. The rate ratio r^0_{ETBE}/r^0_{TAEE} was about 4.4 for the high active resins, 3.8 for medium active resins and 3.4 for low active resins.

The obtained TOF^0_i values for each resin, particularly for ETBE reaction, are larger than those typically reported in the dehydration of C_3-C_8 linear alcohols using the same catalysts,[1,7,8] which can be due to the inhibiting effect of alcohols and to clusters formation, since the initial alcohol content, and consequently the effect of swelling, is larger in dehydration reaction systems. Generally, the etherification rates rank observed was maintained in terms of TOF^0_i values. Nevertheless, TOF^0_i values for resin CT-124 were remarkably low, being almost the same of A-46, the resin with the lowest acid capacity. As stated, despite having a relatively high acid capacity, the absence of permanent pores in CT-124 resin influences therefore the relative efficiency of active sites detrimentally making them to work at low efficiency, which can be ascribed to accessibility limitations. The same explanation can be attributed to the low TOF^0_i values obtained

for A-39. With respect to the low TOF^0_i values obtained for MN-500, its very rigid structure impedes the swelling of microspheres and this could affect the diffusion of molecules and therefore accessibility of reactants to the gel-phase where active sites are located.

3.5 Relations between catalytic activity and morphological properties

As all IER are active in the studied etherification reactions, the relation between catalytic activity and sulfonic groups concentration is self-evident. However, there are more factors of structural nature, such as accessibility, that affect catalytic activity. The response surface methodology (RSM) can be applied to identify which independent variables affect significantly a response variable by means of a polynomial fit. For most processes, a second order response surface is accurate enough for describing nonlinear relationship between variables and measured responses.[25] As for the independent variables, the acid capacity and the catalyst properties from Table 3 (separately for those obtained in dry state from BET isotherms and those obtained in swollen polymer state from ISEC) have been considered. Because of the aforementioned anomalies obtained for A-40, it was decided to dismiss this resin for the analysis. The following general second order polynomial that includes second order interactions has been considered:

$$y = \beta_0 + \sum_{m=1}^{n} \beta_m z_m + \sum_{m=1}^{n} \beta_{mm} z_m^2 + \sum_{l=1}^{n} \sum_{m=l+1}^{n} \beta_{lm} z_l z_m \qquad (5)$$

where z_1, z_2, …, z_n are the coded independent variables (linearly scaled between –1 to 1), y is the response variable, and β_0, β_m, β_{mm} and β_{lm} are fitting parameters. The response variable refers to the catalytic activity. It has been evaluated as the initial reaction rate, because reaction rates present the largest value at that instant, which is of interest to obtain the better resolution of the effect of the resin properties. According to the experimental procedure, at the start of the experimental run the dry resin was injected into the reactor and, subsequently, a sample was taken to be analysed. When the resin comes in contact with the reaction medium, the dry resin accommodates its morphology to that medium. It has been observed that this accommodation proceeds rapidly, because in all experiments, similarly to the one presented in Figure 4, the initial points match correctly in the whole evolution of the species concentration. As a consequence, it has been assumed that this initial accommodation does not affect the reliability of the estimated initial reaction rates. A confidence level of 95% was used to assess the statistical significance of fitted polynomial models evaluated by the test of Fisher (F-value). The number of variables of Eq. 5 was reduced to the minimum statistically significant by means of the stepwise regression procedure[26] using the software Design-Expert 10. The significance level for each parameter to be either included or rejected from the final equation was evaluated by its p-value for a 95% of probability level (p=0.05). In a first attempt, the response variable was the initial reaction rate for each etherification reaction, r^0_{ETBE} and r^0_{TAEE}. In this case, residuals showed an important increasing spread with the calculated values, what indicated a non constant variance of the residuals (heteroscedasticity). Since in RSM it is advisable that the residuals present a constant variance (homoscedasticity), a transformation on the response variable has been considered, being the square root of initial reaction rates, based on the results obtained from Box Cox power transformations method.[27]

The statistical results from RSM expressed in terms of coded variables are gathered in Table 6. The parity plot of experimental data vs. predicted values confirms the suitability of the fitted equations, and residuals plot confirms the randomness of the residuals for each model (Fig. 7). Outcomes reveal that a lineal polynomial function without interactions fits satisfactorily to experimental data. The catalytic activity is better correlated with physicochemical and ISEC properties of the catalyst rather than with dry state properties, since no significant correlation was found for catalytic activity with any dry state property. This is coherent because, as seen in volumetric swelling experiments and in agreement with the literature,[16] IER swell similarly in EtOH and in water. Therefore, ISEC properties should be more representative of the actual working-state of the catalyst in the studied etherification reactions.

The analysis of variance (ANOVA) indicates that the proposed empirical models are adequate to express the actual relation between responses and significant variables with large values of adjusted R^2 (>0.95). Acid capacity and V_{sp} are the only significant variables in the proposed models for both r^0_{ETBE} and r^0_{TAEE}. The coincidence of the equation form is coherent, since both ethers are produced through analogous reactions. The goodness of fit was slightly better for TAEE than for ETBE. The largest divergences in the fitting of empirical equations were found for initial etherification rates obtained on A-36 and A-DT. Eqs. 6 and 7 show the empirical relations equivalent to the obtained with the RSM, but expressed in terms of non-coded variables, for practical purposes. The positive parameter values for the acid capacity and the negative ones for the volume of swollen polymer indicate that catalytic activity of IER can be directly related to the ratio $[H^+]/V_{sp}$. In effect, both plots of r^0_{ETBE} and r^0_{TAEE} vs the ratio $[H^+]/V_{sp}$, show a linear trend for each etherification. Consequently, resins with high concentration of sulfonic groups and with low volume of swollen polymer are the best option for the simultaneous production of ETBE and TAEE. A high concentration of sulfonic groups in a reduced space can allow clusters formation or coordination of active sites that eventually boost etherification reactions. This result also enforces that crosslinking degree and macropores play a determinant role, since they make the permeation of molecules easier and thereby the ensuing accessibility to active sites. Examples of IER with such combination of features are those macroreticular oversulfonated with high crosslinking degree as A-35, A-48 and CT-275.

$$\left(r^0_{ETBE}\right)^{0.5} = (3.16 \pm 1.05) + (3.19 \pm 0.22)[H^+] - (6.03 \pm 0.74) V_{sp} \qquad (6)$$

$$\left(r^0_{TAEE}\right)^{0.5} = (1.72 \pm 0.41) + (1.42 \pm 0.08)[H^+] - (2.48 \pm 0.29) V_{sp} \qquad (7)$$

Table 6 Fitted parameters values and statistical properties of the significant coded variables for the empirical models obtained from the response surface methodology.

Terms	$(r^0_{ETBE})^{0.5}$			$(r^0_{TAEE})^{0.5}$		
	Coefficient	*p*-value	standard error	Coefficient	*p*-value	standard error
β_0	6.21	$1.42\cdot10^{-8}$	0.42	3.31	$4.64\cdot10^{-10}$	0.16
β_1 ([H$^+$])	7.58	$1.31\cdot10^{-8}$	0.51	3.36	$3.01\cdot10^{-9}$	0.20
β_2 (V_{sp})	-4.15	$5.79\cdot10^{-6}$	0.51	-1.17	$3.13\cdot10^{-6}$	0.20
Adjusted R^2		0.95			0.96	
Model *F*-value		118.15			153.26	
Critical *F*-value		$3.62\cdot10^{-8}$			$9.29\cdot10^{-9}$	

Equations 6 and 7 can be useful for designing new catalysts with a larger [H$^+$]/V_{sp} ratio with the aim of assessing whether catalytic activity in etherification reactions can be increased. Since the acid capacity depends on the sulfonation degree of the polymer, which is limited by the number of benzene rings, and V_{sp} depends on the crosslinking degree, the existence of a threshold or optimum value of [H$^+$]/V_{sp} could be somehow expected.

As for the present reaction system the initial mixture is composed by EtOH and olefins ($R°_{A/O}$) = 1.1, the reaction mixture is undergoing a transition towards a less polar environment as reaction time increases, owing to EtOH consumption to form ethers (non-polar compounds). Consequently, resins should experience some shrinking effect as reactions proceed. Catalytic activity has been measured as initial reaction rates, when the reaction medium is more polar. Therefore, IER are more swollen at initial reaction times, and ISEC properties should describe more reliably the initial actual catalyst working-state, in agreement with the results obtained. However, it can be inferred that resins do not swell in the same degree as it could be expected in pure water or pure EtOH. ISEC data provides information on the catalysts morphological properties when totally swelled in water and thus, the actual structural properties are somehow different in the present reaction system of lower polar nature. Nevertheless, it can be assumed that the specific volumes of swollen polymer described by ISEC maintain their relative identity despite the mentioned differences in the reaction media polarity. The good correlation found between catalytic activity and volume of swollen polymer enforces this assumption.

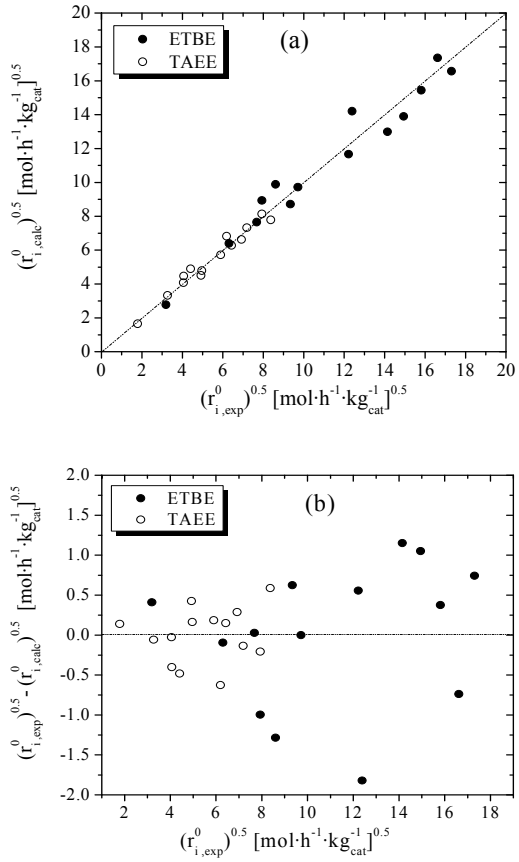

Figure 7 (a) Predicted etherification rates vs. experimental ones for ETBE and TAEE. (b) Residual plots for ETBE and TAEE reaction rates

4. Conclusions

Swelling of a resin is influenced by the nature of the bulk phase and by the resin properties, such as crosslinking degree and acid capacity. Observed swelling in methanol and ethanol is comparable to that in water. All the tested resins are active and highly selective in the simultaneous synthesis of ETBE and TAEE. The outstanding values of reactants selectivity towards ethers obtained for the most active IER make the process

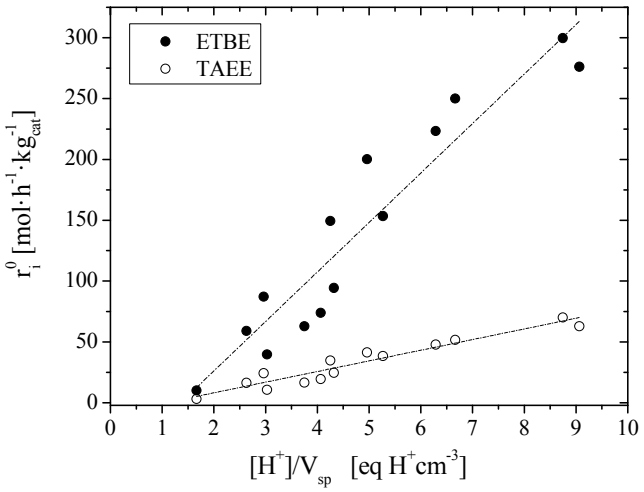

Figure 8 r^0_i vs. ratio of acid capacity to volume of swollen polymer

industrially attractive, as well as the selected experimental conditions suitable for the simultaneous production of ETBE and TAEE.

Macroreticular oversulfonated resins show the best performance in the present reaction system, among them Amberlyst™35 being the most active catalyst. RSM has been used to obtain empirical equations that correlate catalyst properties with the observed catalytic activity. Swollen state properties show better correlation with catalytic activity than dry state properties. In the simultaneous production of ETBE and TAEE, the highest activity has been found for resins with high acid capacity and low volume of swollen polymer.

Acknowledgements

The authors thank The Dow Company and Purolite for providing the ion-exchange resins used in this work. The authors would like to express their gratefulness to Dr. Karel Jeřábek from the Institute of Chemical Process Fundamentals (Academy of Sciences of the Czech Republic) for providing the ISEC morphological analysis of the resins. There are no conflicts of interest to declare.

Nomenclature

2M1B	2-methyl-1-butene
2M2B	2-methyl-2-butene
BET	Brunauer, Emmett and Teller
BJH	Barrett, Joyner and Halenda
d_{pore}	pore diameter [nm]
ETBE	ethyl *tert*-butyl ether
EtOH	ethanol
IB	isobutene
ISEC	Inverse Steric Exclusion Chromatography
n_k	mole of product *k* formed
r^0_i	intrinsic initial rate of reaction *i*, [mol $(kg_{cat}\cdot h)^{-1}$]
r_i	intrinsic rate of reaction *i*, [mol $(kg_{cat}\cdot h)^{-1}$]
$R°_{A/O}$	initial ratio alcohol to olefins [dimensionless]
$R°_{C4/C5}$	initial ratio C_4 to C_5 olefins [dimensionless]
$S_{g,BET}$	surface area determined by BET or ISEC [$m^2\cdot g^{-1}$]
S_j^k	selectivity of reactant *j* towards product *k* [%]
SR	swelling ratio [dimensionless]
t	reaction time [min]
T	temperature [K]
TAA	*tert*-amyl alcohol
TAEE	*tert*-amyl ethyl ether
TBA	*tert*-butyl alcohol
TOF	turnover frequency of the catalyst [mol $(h\cdot eq\ H^+)^{-1}$]
V_{pore}	pore volume determined by BET or ISEC [$cm^3\cdot g^{-1}$]
V_{sp}	true volume of swollen polymer [$cm^3\cdot g^{-1}$]
W_{cat}	catalyst mass in dry basis [g]
X_j	conversion of reactant *j* [%]
Y_j^k	yield of reactant *j* towards product *k* [%]
θ	porosity [%]
ρ	skeletal density [$g\cdot cm^{-3}$]

References

1 C. Casas, R. Bringué, E. Ramírez, M. Iborra and J. Tejero, *Appl. Catal., A*, 2011, **396,** 129–139.
2 B. M. Antunes, A. E. Rodrigues, Z. Lin, I. Portugal and C. Silva, *Fuel Process. Technol.*, 2015, **138,** 86–99.
3 R. L. Albright, *React. Polym., Ion Exch., Sorbents*, 1986, **4,** 155–174.
4 K. Jeřábek, L. Hankova and A. Revillon, *Ind. Eng. Chem. Res.*, 1995, **34,** 2598–2604.
5 J. Guilera, E. Ramírez, C. Fité, J. Tejero and F. Cunill, *Catal. Sci. Technol.*, 2015, **5,** 2238–2250.
6 S. Sterchele, P. Centomo, M. Zecca, L. Hanková and K. Jeřábek, *Microporous Mesoporous Mater.*, 2014, **185,** 26–29.
7 R. Bringué, E. Ramírez, M. Iborra, J. Tejero and F. Cunill, *J. Catal.*, 2013, **304,** 7–21.
8 M. A. Pérez, R. Bringué, M. Iborra, J. Tejero and F. Cunill, *Appl. Catal., A*, 2014, **482,** 38–48.
9 R. González, PhD thesis, Univ. Barcelona, 2011.
10 M. Umar, A. R. Saleemi and S. Qaiser, *Catal. Commun.*, 2008, **9,** 721–727.
11 J. H. Badia, C. Fité, R. Bringué, M. Iborra and F. Cunill, *Top. Catal.*, 2015, **58,** 919–932.
12 R. Soto, C. Fité, E. Ramírez, R. Bringué and F. Cunill, *Chem. Eng. J.*, 2017, **307**, 122-134.
13 R. Soto, C. Fité, E. Ramírez, J. Tejero and F. Cunill, *Catal. Today*, 2015, **256,** 336–346.
14 L. Domingues, C. I. C. Pinheiro, N. M. C. Oliveira, J. Fernandes and A. Vilelas, *Ind. Eng. Chem. Res.*, 2012, **51,** 15018–15031.
15 M. Di Girolamo and D. Sanfilippo, in *Sustainable Industrial Processes*, ed. F. Cavani, G. Centi, S. Perathoner and F. Trifiro, Wiley-VCH, Weinheim, 1st edition, 2009, ch. 11, 469
16 E. Van de Steene, J. De Clercq and J. W. Thybaut, *J. Ion Exch.* (2014) **25,** 234–241.
17 B. Corain, M. Zecca and K. Jeřábek, *J. Mol. Catal. A: Chem.*, 2001, **177,** 3–20.
18 U. Kunz, C. Altwicker, U. Limbeck and U. Hoffmann, *J. Mol. Catal. A: Chem.*, 2001, **177,** 21–32.
19 S. Lowell and J. E. Shields, *Powder Surface Area and Porosity*. Springer, Amsterdam, 1991.
20 G. Leofanti, M. Padovan, G. Tozzola and B. Venturelli, *Catal. Today*, 1998, **41,** 207–219.
21 M. Umar, D. Patel and B. Saha, *Chem. Eng. Sci.*, 2009, **64,** 4424–4432.
22 A. G. Ogston, *Trans. Faraday Soc.*, 1958, **54,** 1754–1757.
23 R. Soto, C. Fité, E. Ramírez, R. Bringué and F. Cunill, *Fuel Process. Technol.*, 2016, **142,** 201–211.
24 R. Soto, C. Fité, E. Ramírez, R. Bringué and F. Cunill, *Chem. Eng. Res. Des.*, 2014, **92,** 644–656.
25 R.H. Myers, D. C. Montgomery, C. M. Anderson-Cook. *Response surface methodology*, John Wiley & Sons, New Jersey, 2009.
26 N. Draper and H. Smith, *Applied Regression Analysis*, John Wiley and Sons, New York, 1981.
27 G. E. P. Box and D. R. Cox. *J. R. Stat. Soc. B*, 1964, **26,** 211–252.